Experimental Study of Quasistatic Brittle Crack Propagation

O. Ronsin, F. Heslot, and B. Perrin

Laboratoire de Physique de la Matière Condensée de l'Ecole Normale Supérieure, 24 rue Lhomond, 75231 Paris Cedex 05, France

(Received 5 May 1995)

This Letter presents an experimental study of controlled brittle crack propagation in thin glass strips, using a thermally induced stress field. For straight and oscillating crack propagation, three regimes are observed, controlled by a set of characteristic lengths. Direct measurements of the thermal field allows meaningful comparison with a model for straight symmetric crack based on two-dimensional elasticity. This strongly supports a *velocity-independent fracture energy*. For the oscillating onset, it is shown that the Cotterell-Rice criterion is not valid here.

PACS numbers: 62.20.Mk, 46.30.Nz

Quasistatic brittle fracture is an old topic [1], which has recently attracted a renewed interest, both experimentally [2] and theoretically [3–5]. By using a thermal field to induce stress [2,6], it is possible to obtain a steady propagating crack, localized within a thermal gradient created between a hot oven and a cold bath. The recent work of Yuse and Sano [2] demonstrated nicely the successive instabilities of such a localized crack.

This Letter presents a detailed experimental study of the onset of straight and oscillating crack propagation over a previously unexplored low-velocity range, along with an analysis of the relevant parameters. A comparison with theoretical predictions based on two-dimensional linear elasticity is successfully performed for straight cracks, and a value of the surface energy γ of the glass is deduced.

The experimental setup, inspired by the work of Yuse and Sano [2] (Fig. 1), has been designed in order to allow low-velocity experiments and long samples. 0.5 to 1 m long soda-lime glass plates of various thicknesses e (0.13, 0.6, and 0.9 mm) and widths L (from 3 to 400 mm) are used. The plate, mechanically scored at the edge to seed the crack, is moved at constant velocity V in the range 0.01 to 10 mm s^{-1} by a translation stage driven by a stepping motor, from a hot to a cold region separated by a distance $h = 3$ to 10 mm. The hot oven consists of a slot of thickness 1.1 mm between two heating elements regulated at a temperature T^+ adjustable between 40 and 250 $\pm$ 0.1 °C. The cold region consists of a bath of circulating water of constant mean level. The circulation is created to maintain a constant temperature T^- of the water, regulated within ± 1 °C over the range 15 to 25 °C. The interface between the glass plate and the water surface may form a meniscus of fluctuating size (capillary length 3 mm). To obtain a better control of the gap h (± 0.1 mm), a constant dynamic contact angle (about 90°) is obtained by silanizing the glass plate [7].

A steady thermal profile is related to the temperature difference $\Delta T = T^+ - T^-$, to the distance h between the two thermostats, and to the driving velocity V, which advects and localizes the thermal gradient near the cold bath over a thermal diffusion length $d_{\text{th}} = D/V$, where D is the thermal diffusion coefficient of the glass (0.47 $mm^2\,s^{-1}$).

This steady thermal regime is reached after an initial transient dependent on both thermal diffusion in the plate and finite heat resistance of the coupling between the temperature baths and the plate. This necessitates a length of at least 50 mm of glass plate for a typical velocity $V = 0.1$ mm s^{-1}.

The temperature field is independent of the width L of the plate, and induces thermal expansion in the sample. But the elastic energy stored in the glass plate for a given thermal field (ΔT, h, and V fixed) depends on L, which is then used as a control parameter. For a given thermal profile $(V, h, \Delta T)$, the crack behavior is studied as a function of the width L: For widths below a critical value L_c, no crack grows. At larger widths, and as long as L stays below another critical width L_{osc}, a straight crack

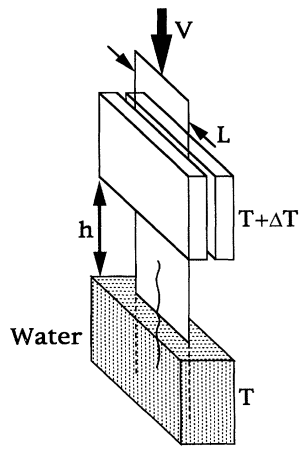

FIG. 1. Schematic setup of the experiment. A cracked glass plate of width L is driven at constant velocity V through a hot oven at temperature $T + \Delta T$ and in a cold bath of water at T. The resulting thermal gradient is imposed by the temperature difference ΔT, the distance h between the two temperature baths, and the driving velocity V. In such a configuration, the crack tip can be trapped in the gradient, enabling the control of the fracture velocity.

 0031-9007/95/75(12)/2352(4)$06.00 © 1995 The American Physical Society

propagates in the middle of the plate at constant velocity $-V$ relative to the plate (the crack tip position is fixed in the thermal field). Above L_{osc}, the crack path becomes wavy, showing very regular oscillations just beyond L_{osc} (inset of Fig. 2) and becoming less and less regular as L is increased, with possible period doubling, rupture of symmetry, and eventually crack nucleation for very large widths. Experimentally, for a given velocity, the first regimes are covered by using a single glass plate of slowly decreasing width (relative variation of width vs length less than 1%).

A typical "phase" diagram in the (L,V) space is obtained and presented in Fig. 2 for $\Delta T = 135$ °C and $h = 5$ mm, showing these "phases" (no propagation, straight propagation, and wavy propagation) separated by the two curves $L_c(V)$ and $L_{osc}(V)$.

Three distinct V dependencies are observed and shown to be related to the characteristic lengths h, e, and D/V (see Fig. 3).

At low velocities ($V < D/h$), the critical width has little dependence on V, the thermal profile being essentially controlled by the gap h which is larger than the thermal diffusion length d_{th}.

The intermediate regime ($D/h < V < D/e$) is related to the advection of the thermal gradient near the cold bath over the length d_{th}. This localization increases the induced stress and a smaller width is needed to obtain a propagating crack.

For large velocities ($V > D/e$), the thermal diffusion length becomes smaller than the thickness of the plate, the temperature is no longer homogeneous across the thickness, and the fracture process becomes three dimensional. This change (2D → 3D) is clearly illustrated on the fracture surface, smooth at low velocity and rough at high velocity.

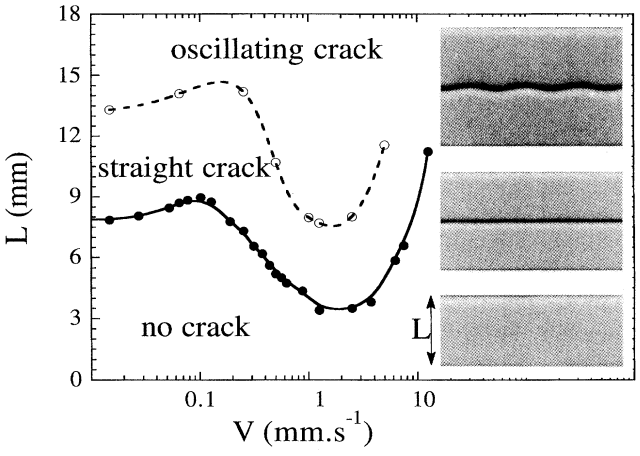

FIG. 2. Phase diagram in the (L,V) control parameter space for a glass plate of thickness $e = 0.9$ mm, with $h = 5$ mm and $\Delta T = 135$ °C. The $L_c(V)$ curve (●) corresponds to the arrest of straight crack propagation, while the $L_{osc}(V)$ curve (○) corresponds to the bifurcation to oscillating crack propagation. Lines are guides to the eye. Cracked glass strips corresponding to the three phases are shown in the inset.

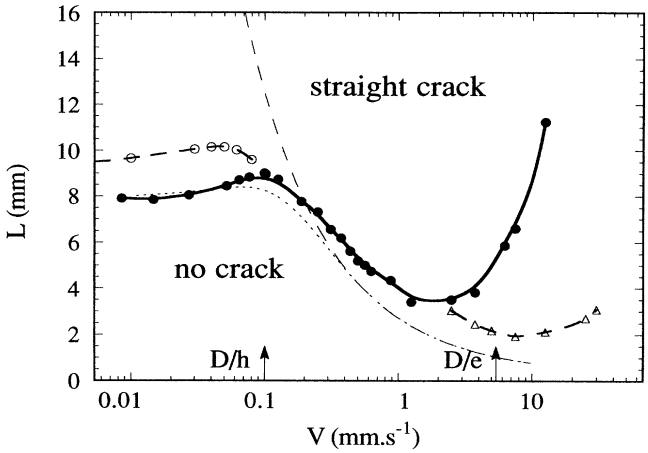

FIG. 3. $L_c(V)$ curve for the first bifurcation: experimental points (●) for $e = 0.9$ mm, $h = 5$ mm, and $\Delta T = 135$ °C; the two arrows correspond to $V = D/h$ and $V = D/e$, separating three regimes of $L_c(V)$ (i) h controlled, (ii) D/V controlled, and (iii) e controlled. The effect on the $L_c(V)$ curves obtained by changing e appears for $e = 0.14$ mm, $h = 5$ mm, and $\Delta T = 135$ °C (△), and by changing h for $h = 10$ mm, $e = 0.9$ mm, and $\Delta T = 135$ °C (○). The thin broken lines (———, - - -) correspond to the theoretical $L_c(V)$ curves, both obtained with a two-dimensional elastic model, using the Griffith criterion and a surface energy $\gamma = 1.6$ J m^{-2}. The curve (———), which diverges at low velocities, is obtained in the nonphysical limit $h \to \infty$. The curve (- - -) is obtained when taking into account the finite value of h. The value of γ is determined so as to get a fit between the experimental and theoretical (- - -) curves at very low velocities.

Let us focus on the two-dimensional low-velocity regimes. It appears that the low-velocity h-controlled transition presents a weak dependence on V. A bump with a maximum L_c^{max} is present in the $L_c(V)$ curves. For a plate of constant width, chosen between $L_c(V = 0)$ and L_c^{max}, the crack cannot propagate in a given range of V. This effect of forbidden velocity gap may be illustrated by studying the dynamics of the crack tip and will be presented in detail elsewhere [8].

Let us compare these experimental results to a two-dimensional linear elastic model. The problem of an infinite elastic strip with a semi-infinite straight crack in its middle with a one-dimensional thermal field applied was first solved by Marder [3], who obtained an analytical expression for the elastic energy G released per unit length of virtual crack propagation and per unit thickness as a function of the crack tip position z_{tip} (G is called the energy release rate). For a given loading condition [thermal profile $T(z)$ and plate's width L], it is then possible to evaluate numerically the energy release rate $G(z_{tip})$, as described in Ref. [3]. Until now, only the theoretical limiting case of infinite gap h was considered, leading to a temperature profile only determined by the

thermal diffusion length d_{th} [3,4]. This assumption of infinite h is not valid anymore for velocities smaller than D/h. In order to extend the range of comparison between theory and experiment to low speeds, we consider a more realistic profile:

$$T(z) = \Delta T\left[\frac{1 - \exp(-z/d_{\text{th}})}{1 - \exp(-h/d_{\text{th}})} \times \theta(z)\theta(h - z) + \theta(z - h)\right], \quad (1)$$

where $\theta(z)$ is the step function.

A corresponding curve of the energy release rate $G(z_{\text{tip}})$ is shown in Fig. 4 for a temperature profile and for three different plates' widths. The condition of propagation is now determined by the Griffith energy balance criterion [1], which consists of the comparison between the elastic energy released G with the energy needed to create the two resulting new surfaces 2γ where γ is the surface energy of the glass. This criterion has been generalized to dynamic crack growth by introducing a velocity dependent phenomenological surface energy [called fracture energy $\Gamma(V)$] to take into account dissipative effects such as plasticity. For $G_{\max} < \Gamma(V)$, where $G_{\max}$ is the maximum of $G(z)$, there is no position of the crack tip where enough elastic energy is released to create the surface, and no propagation is possible. For $G_{\max} > \Gamma(V)$, there are two equilibrium positions for the crack tip, but only the one near the hot bath (for which $dG/dz < 0$) is stable. Steady crack propagation stops when $G_{\max} = \Gamma(V)$, which corresponds to the critical value $L_c(V)$.

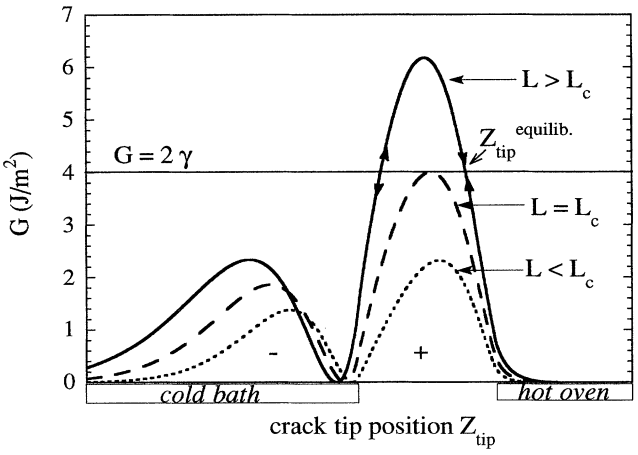

FIG. 4. Typical dependence of the energy release rate G vs the crack-tip position z_{tip}, calculated for a given thermal profile (ΔT, h, and V fixed) for three different sample widths. The part in the cold bath (with a minus sign) corresponds to a compression of the crack faces on each other. This state is of no physical interest because the model supposes stress-free boundaries. The application of the Griffith criterion gives the equilibrium position of the crack tip as the intersection of the curve $G(z_{\text{tip}})$ with the horizontal line $G = 2\gamma$. A minimum sample width L_c is necessary for crack propagation, when the maximum $G_{\max}$ of $G(z_{\text{tip}})$ equals 2γ. For $L < L_c$, the crack cannot propagate. For $L > L_c$, two equilibrium positions are possible for the crack tip; the stable one is in the decreasing part of $G(z_{\text{tip}})$.

The theoretical curve $L_c(V)$ thus depends on Γ, which is unknown. We will first assume that $\Gamma(V)$ is a constant, equal to the also unknown static value γ. Using the assumed temperature profile (1), and adjusting the value of γ so that the theoretical value of L_c at low velocity (typically 0.01 mm s^{-1}) fits the experimental data, we find $2\gamma = 3.2$ J m^{-2}, assuming a Young modulus of $E = 7.2 \times 10^{10}$ J m^{-3} and a linear coefficient of thermal expansion of $\alpha = 0.77 \times 10^{-5}$ K^{-1} for glass. The curve $L_c(V)$ calculated in this case [$\Gamma(V) = \text{const} = 2\gamma = 3.2$ J m^{-2}] is plotted in Fig. 3, also showing the limiting case $h \to \infty$. The agreement is qualitatively good, and, in particular, we recover the bump at low velocities, which can thus be understood on the basis of this model: Since a uniform temperature gradient gives rise to no stress in a free sample [9], stresses in the glass plate are induced by the curvature of the temperature field. This stress field extends over a length that scales with the width of the plate. A crack is attracted towards regions of negative curvature ($\partial^2 T/\partial z^2 < 0$) and is repelled by positive ones (the crack faces tend, respectively, to be forced open or forced closed). For $V = 0$, strong curvature is localized near $z = h$ (where $\partial^2 T/\partial z^2 < 0$), and corresponds to a strong $G_{\max}$. As V is increased, but still small compared to D/h, the negative curvature field is advected and smoothed. The effect is a decrease of $G_{\max}$. Higher velocities localize and increase negative curvature near the temperature boundary $z = 0$. The effect is a reincreasing of $G_{\max}$; the crack tip then stabilizes near the cold bath. For certain values of L, this variation of the maximum of G will cross the constant critical value 2γ, prohibiting propagation within a band of velocities.

The discrepancy between the experimental data and the predictions of the model may be attributed to the use of a constant surface energy γ, which cannot account for eventual crack velocity-dependent dissipation. If now, for each experimental point of the $L_c(V)$ curve, the fracture energy Γ is adjusted so as to make the theoretical point coincide with the experimental one, the procedure leads to a velocity dependence of Γ, shown in Fig. 5. However, a more plausible way to interpret the data is first to question the validity of the assumed ideal temperature profile. This profile (perfect baths) overestimates the second derivatives (it assumes discontinuities of the first derivatives of the temperature at $z = 0$ and $z = h$), and the above adjustment for Γ thus overestimates the value of the fracture energy. The real thermal profiles have been measured experimentally for thick plates ($e = 0.9$ mm). A thermocouple is inserted and glued inside a 0.35 mm diameter hole drilled into the side of the thickness of the plate, with a depth of 5 mm. The temperature profiles measured for $V < 0.3$ mm s^{-1} show that the thermostats

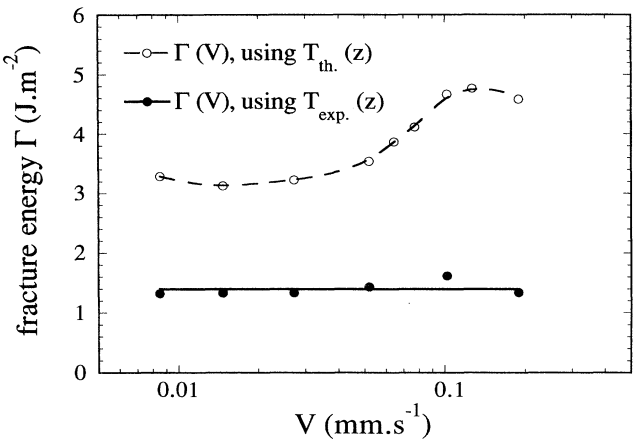

FIG. 5. Fracture energy of the glass sample as a function of the crack velocity, extracted from the experimental threshold for propagation, using an idealized (○) or experimental (●) temperature profile. The use of the real temperature profile leads to a *velocity-independent fracture energy*, i.e., a surface energy of $\gamma = 0.7 \pm 0.2\ \mathrm{J\,m^{-2}}$.

are not perfect: no discontinuity of the gradient at $z = 0$ and h is observed. Instead, around $z = 0$ ($z = h$), a smooth change of the temperature over a characteristic distance of 1 mm (2 mm) is measured. This is related to the thermal impedance of both temperature baths. These profiles were fitted with analytical functions and included in the model. The resulting values for the fracture energy as a function of the velocity are plotted in Fig. 5 and have been checked to be independent of the temperature difference ΔT between the two baths. This now gives a *fracture energy that is independent of the crack velocity* (up to the experimental precision). This constant value over more than one decade of velocities can thus be considered as the surface energy of the glass $\gamma = 0.7\ \mathrm{J\,m^{-2}}$, and is not unreasonable with respect to quoted values in the literature, measured directly [1] or based upon interpretation of nonsteady crack propagation [10]. This constant value of γ was checked to be consistent with the measurements of the equilibrium crack tip position between the hot and cold baths [8].

For the oscillatory threshold $L_{\mathrm{osc}}(V)$, the striking similarity between the $L_c(V)$ and $L_{\mathrm{osc}}(V)$ experimental curves suggests that, as for the description of the three different regimes for straight cracks, the instability mechanism is related to stresses induced by the thermal field, and so that the same characteristic lengths are involved to separate various regimes.

The velocity-independent fracture energy has been obtained here in the case of straight cracks, where the two-dimensional elastic model restricted to symmetric loading conditions (straight crack path in the middle of the sample) should rightfully apply. However, analyzing the oscillation threshold (experimental data of Ref. [2]), Marder [3] extracted a fracture energy rapidly decreasing with the velocity ($50\ \mathrm{J\,m^{-2}}$ drop in fracture energy for an increase in velocity of $1\ \mathrm{mm\,s^{-1}}$). This result was based on the path stability criterion of Cotterell and Rice (CR) for straight symmetric cracks [11]. To check this criterion with the present data and with the measured temperature profile, we have performed similar calculations. Using the previously determined value of $\gamma = 0.7\ \mathrm{J\,m^{-2}}$, this criterion gives values of L_{osc} no more than 5% higher than the corresponding L_c, instead of the measured 70%. The CR criterion does not hold here, in the present geometry. This may be due to the infinite medium assumption used to derive it. Other criteria [4,5] have recently been proposed, but further work using the real experimental thermal profile will be needed to check their compatibility with the present experiment.

The work presented here strongly supports a coherent interpretation of the experimental data on straight crack propagation in terms of (i) a constant surface energy γ, and (ii) a set of characteristic lengths. The measurement of the real experimental temperature profile is essential to get a meaningful comparison between the experiment and the theory. The study of the oscillations demonstrates that the onset does not follow the Cotterell-Rice criterion. The physical understanding of this instability may now be attacked from a firm basis, with the successful description of straight crack propagation.

We would like to acknowledge T. Baumberger for helpful discussions and M. Marder for kindly transmitting some data concerning the numerical results of his work [3]. The Laboratoire de Physique de la Matière Condensée is "associé au Centre National de la Recherche Scientifique (CNRS), et aux Universités Paris VI et Paris VII."

[1] A. A. Griffith, Philos. Trans. R. Soc. London Ser. A **221**, 163 (1920).
[2] A. Yuse and M. Sano, Nature (London) **362**, 329 (1993).
[3] M. Marder, Phys. Rev. E **49**, R51 (1994).
[4] S. Sasa, K. Sekimoto, and H. Nakanishi, Phys. Rev. E **50**, R1733 (1994).
[5] M. Adda-Bedia and Y. Pomeau (to be published).
[6] M. Hirata, Sci. Pap. Inst. Phys. Chem. Res. (Jpn.) **16**, 172 (1931).
[7] Sigmacote, Sigma Chemical Co.
[8] O. Ronsin, F. Heslot, and B. Perrin (to be published).
[9] S. P. Timoshenko and J. N. Goodier, *Theory of Elasticity* (McGraw-Hill, New York, 1982), 3rd ed.
[10] S. M. Wiederhorn, in *Mechanical and Thermal Properties of Ceramics,* edited by J. B. Watchman, NBS Special Publication No. 303 (U.S. GPO, Washington, DC, 1969), p. 217.
[11] B. Cotterell and J. R. Rice, Int. J. Fract. **16**, 155 (1980).

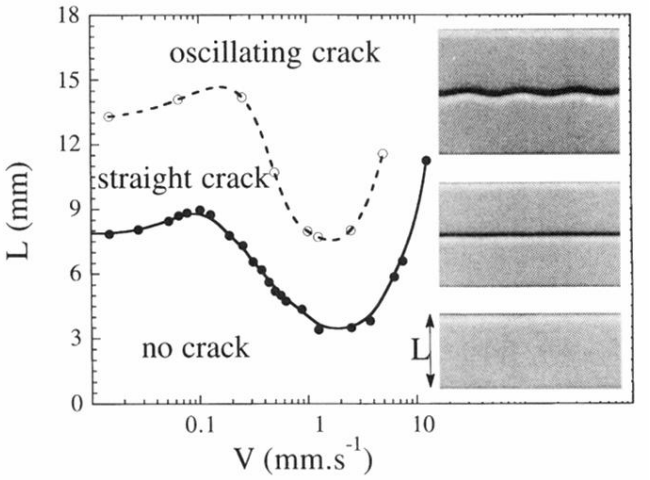

FIG. 2. Phase diagram in the (L,V) control parameter space for a glass plate of thickness $e = 0.9$ mm, with $h = 5$ mm and $\Delta T = 135\,^{\circ}\mathrm{C}$. The $L_c(V)$ curve (●) corresponds to the arrest of straight crack propagation, while the $L_{\mathrm{osc}}(V)$ curve (○) corresponds to the bifurcation to oscillating crack propagation. Lines are guides to the eye. Cracked glass strips corresponding to the three phases are shown in the inset.